A Smart Sensor Web for Ocean Observation: Integrated Acoustics, Satellite Networking, and Predictive Modeling

Bruce M. Howe*, Nathan Parrish†, Leonard Tracy†, Andrew Gray†, Yi Chao‡,
Tim McGinnis*, Payman Arabshahi*, Sumit Roy†

*Applied Physics Laboratory, Box 355640, University of Washington, Seattle, WA, 98105
†Dept. of Electrical Engineering, Box 352500, University of Washington, Seattle, WA 98195
‡ JPL/UCLA Joint Institute for Regional Earth System Science and Eng., University of California, Los Angeles, 9258 Boelter Hall, Los Angeles, CA 90095

***Abstract* – In many areas of Earth science, including climate change research, there is a need for near real-time integration of data from heterogeneous and spatially distributed sensors, in particular in-situ and space-based sensors. The data integration, as provided by a smart sensor web, enables numerous improvements, namely, 1) adaptive sampling for more efficient use of expensive space-based sensing assets, 2) higher fidelity information gathering from data sources through integration of complementary data sets, and 3) improved sensor calibration. The specific purpose of the smart sensor web to be demonstrated as part of the development presented here is to provide for adaptive sampling and calibration of space-based data via in-situ data. Our ocean-observing smart sensor web presented herein is composed of both mobile and fixed underwater in-situ ocean sensing assets and Earth Observing System (EOS) satellite sensors providing larger-scale sensing. An acoustic communications network forms a critical link in the web between the in-situ and space-based sensors and facilitates adaptive sampling and calibration. After an overview of primary design challenges, we report on the development of various elements of the smart sensor web. These include (a) a cable-connected mooring system with a profiler under real-time control with inductive battery charging; (b) a glider with integrated acoustic communications and broadband receiving capability; (c) satellite sensor elements; (d) an integrated acoustic navigation and communication network; and (e) a predictive model via the Regional Ocean Modeling System (ROMS). Results from field experiments as well as simulation and theoretical studies on acoustic communication system performance, link capacity computation, and development of a media access control (MAC) layer protocol for underwater networking, are described. Plans for future adaptive sampling demonstrations using the smart sensor web are also presented.**

I. Introduction

As the effects of global warming and associated climate change become more pronounced, it will be ever more important to accurately know the state of the ocean and to be able to predict it significantly into the future. Earth's oceans however, are clearly undersampled. Efforts are underway to rectify this situation. On global scales, the Integrated Ocean Observing System has deployed drifting, profiling floats around the world to provide (incoherent) in-situ temperature and salinity data. Numerical modeling is only now reaching the state of being able to assimilate this data, as well as satellite altimetry and other data, to produce a 4-dimensional ocean state that is dynamically consistent. However, there are still major discrepancies when one looks at the total heat and fresh water budget [1] – various models and independent data driven results for the fraction of sea level rise attributable to ocean thermal expansion and to ice melting are inconsistent within their respective formal error bars. In another effort, the National Science Foundation has initiated the Ocean Observatories Initiative to provide the leading edge infrastructure for long-term sustained observations. There are many other efforts to develop and sustain long-term ocean observing capability, to complement the satellite data collected by NASA and other space based Earth observing systems.

In this work we are developing a smart sensor web that combines many of the essential elements of an ocean observing system: a mix of fixed and mobile in-situ sensors and satellite sensors that together can perform a combination of spatial and temporal sampling; and an ocean model, embodying all our best and current knowledge of the physics, embedded in a data assimilation framework, that can be used in an adaptive sampling mode to jointly optimize sampling and resource allocation for improved science data. For all the pieces to work together, the power, communications, and timing network infrastructure must be in place; these form a critical link in the web between the in-situ and space-based sensors.

Constructing and demonstrating such a sensor web is a major task, and is only possible within the scope of this project by building on the efforts of several complementary projects: (a) cabled, profiler mooring (ALOHA-MARS Mooring system, http://alohamooring.apl.washington.edu) intended for the NSF Ocean Observatories Initiative, (b) acoustic Seagliders with integrated sensors and modems talking to each other and other platforms, including bottom nodes and gateway buoys, (c) satellite sensors, (d) network infrastructure to integrate the data and information from a-c, and (e) a predictive model via the Regional Ocean Modeling System (ROMS). The system composed of the above is illustrated in Fig. 1. It should be noted that the glider and mooring systems described here are but one of many variants. For example propeller-driven autonomous undersea vehicles (AUVs) transiting between bottom nodes are regarded as conceptually very similar.

II. Smart Sensor Web

A. Mooring sensor system

The basic mooring system is illustrated in Figure 1. The hardware implementation is currently deployed and operating on the Seahurst Observatory in 40 m water depth in Puget Sound, just west of Sea-Tac International Airport. (originally it was supposed to be deployed at the ALOHA Cable Observatory site 100 km north of Oahu in 5,000 m water depth, and then at the MARS observatory in Monterey at 1000 m water depth; however delays at these sites have prevented the deployments).

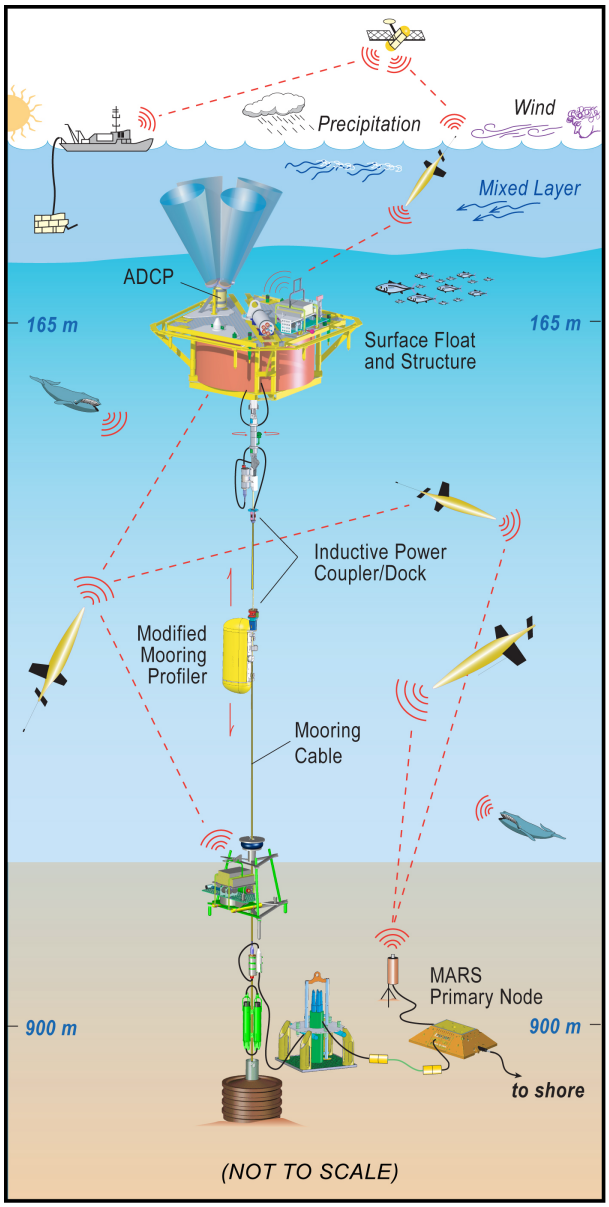

Figure 1: The ALOHA-MARS mooring system, using acoustic Seagliders to extend the spatial sampling footprint.

The basic concept is to provide the infrastructure to distribute power, communications, and precise and accurate timing throughout the water column. An electro-optical-mechanical mooring cable connects the seafloor node to the subsurface float node. Here instrument packages can be connected using underwater-mateable connectors (using a remotely operated vehicle (ROV), or divers if shallow enough). In addition, power is transferred through an inductive coupler (~200 W) to the vertically mobile profiler to charge its batteries; this process is about 70% efficient and lets the profiler run with a 95% duty cycle. Ethernet is used in the mooring system. An inductive modem is used to communicate between the float node and the profiler while it is both stationary and moving (a future upgrade in the profiler software will permit real-time adaptive sampling). Timing is distributed throughout the mooring with a GPS-synchronized pulse-per-second – PPS – signal (a new inductive modem modification will allow a PPS signal to be transferred to the profiler as well).

Sensors at the base of the mooring include dual conductivity, temperature, and depth (CTD) with oxygen, an optical backscatter sensor, and an acoustic modem. The same is on the subsurface float; the profiler has a single CTD and backscatter sensor. On the subsurface float are an acoustic Doppler current profiler (ADCP, measures horizontal velocity as a function of range to the surface, 200 m range for the 150 kHz system) and a broadband (5 Hz – 30 kHz) hydrophone. In addition, the profiler has an acoustic current meter (using local, multiple travel time measurements).

The subsurface float is shown in Fig. 2 on the fantail of the R/V *Thompson* ready for deployment at Seahurst. The large syntactic foam float keeps the mooring cable taut; at Seahurst it is at a nominal depth of 10 m; in the open ocean scenario, it would be at 165 m water depth. On top of the float, one can see the ADCP on the left, the float node cylinder in the middle, and the instrument package on the right. The design is such as to enable easy ROV access to the instrument packages (there are bays for two additional units). The float sits on a trolley on the deck track system, which facilitates deployment. The Woods Hole Oceanographic Institution (WHOI) micromodem is in the instrument package on the outboard side.

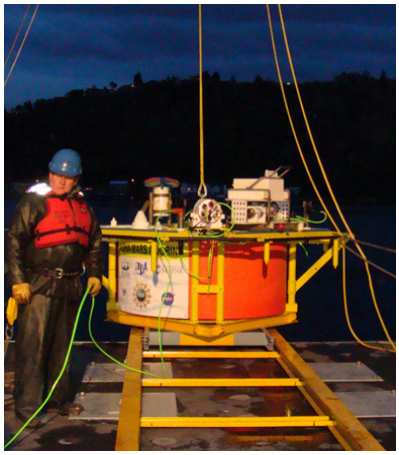

Figure 2: Subsurface float with ADCP, node, and instrument package ready for deployment.

The profiler is shown in Fig. 3. The inductive power coupler (both the primary and secondary coils, shown here mated) is at the top with a limit indicator switch. In the middle is the acoustic current meter (ACM), with the $CTDO_2$ and BB2F optical backscatter sensor just below. Below these is the inductive modem ferrite ring (in white plastic) for real time communications between the profiler and the outside world.

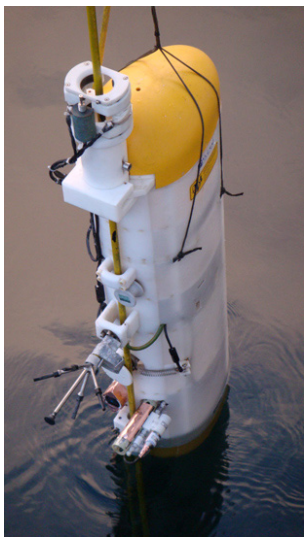

Figure 3: The McLane moored profiler (MMP) modified with an inductive power coupler.

Figure 4 shows the float assembly being deployed. The mooring system was successfully deployed just as this paper was being prepared, but data (such as acoustic communications versus range) has not yet been collected.

During the deployment cruise, multi-beam swath bathymetry was collect in the area; see Fig. 5. This will allow us to perform quantitative acoustic communications performance predictions [2], as well as serving as more precise topographic boundary conditions for the ocean modeling component of our work.

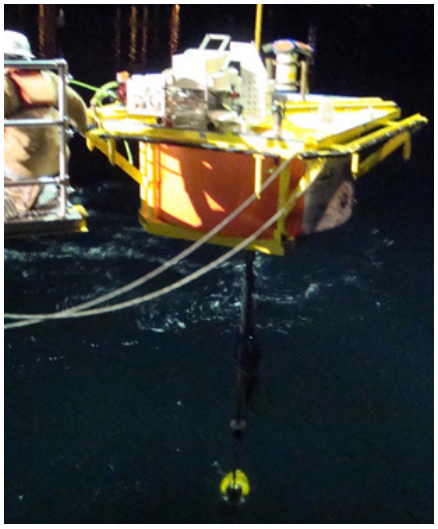

Figure 4: The float being deployed, with the top of the MMP in the water, just visible.

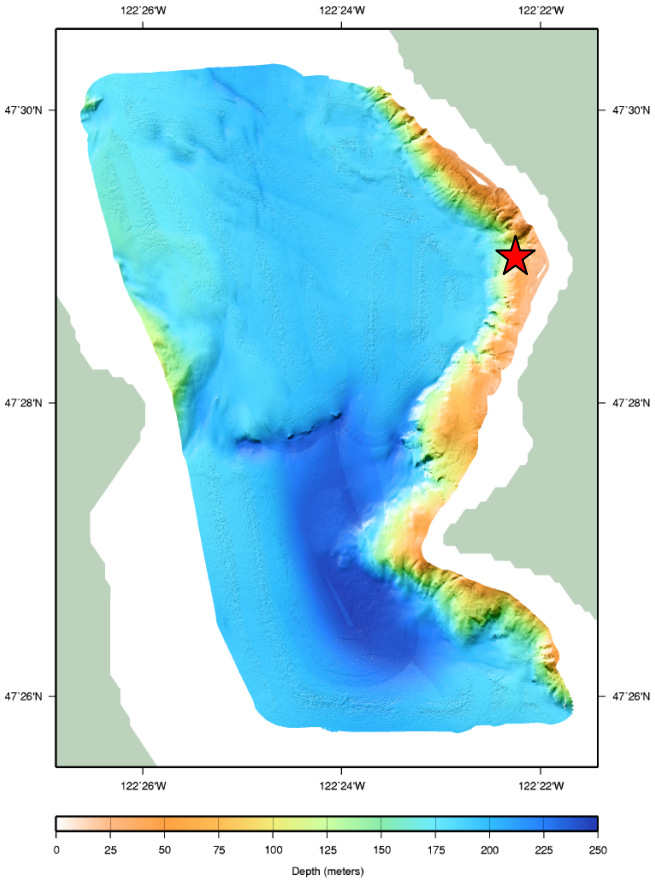

Figure 5: Bathymetry in the vicinity of the Seahurst Observatory and the mooring (star).

B. Seaglider

The basic Seaglider developed at the University of Washington's Applied Physics Laboratory (UW/APL) can dive to 1000 m while moving horizontally at about ½ knot using ½ W of power. Glider missions have now exceeded 600 dives, covering 3,000 km over ground. Gilders routinely collect temperature and conductivity (salinity) data during a dive.

The Seaglider has now been adapted to carry a broadband hydrophone (10 Hz – 30 kHz) and a WHOI acoustic micromodem; see Figs. 6 and 7. The latter operates in the 23 – 27 kHz band.

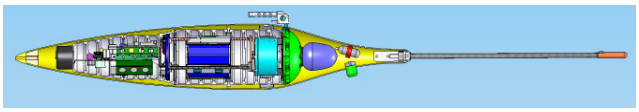

Figure 6: The acoustic Seaglider. The hydrophone is in tail at the top, the acoustic modem transducer beneath it.

Work has proceeded in testing acoustic communications between gliders and between gliders other platforms, both fixed and mobile, at the surface, in the water column, and on the bottom. In one such test in Puget Sound, a glider sat on the bottom and communicated with a glider moving out in

range; see Fig. 8. Frequency shift-key (FSK) signal coding at 80 bits per second (b/s) was used, with reliable results to 4 km and less reliable results to 7 km. In another test, an acoustic modem was installed on a bottom node at 30 m water depth as part of the mooring testing at the Seahurst Observatory in Puget Sound (just west of Sea-Tac airport). Using a boat deployed transducer and deck box, ranges to 2.5 km were obtained (see Fig. 9); the lower ranges than in the first mentioned test were likely a result of the much shallower bottom. In more recent testing, phase-shift-key (PSK) signal coding (coherent vs. the incoherent FSK) was used. In this case 240 b/s and 5200 b/s were obtained between a glider and a surface gateway buoy with a modem suspended beneath; this modem has a 4-element hydrophone-receiving array. Further, a go-to-surface command was sent to the glider to demonstrate real-time vehicle control via the acoustic communications channel. In all cases, one-way travel times were obtained from which range is obtained. In summary, these test results confirm that the acoustic modem can perform adequately both from a communications perspective as well as for navigation.

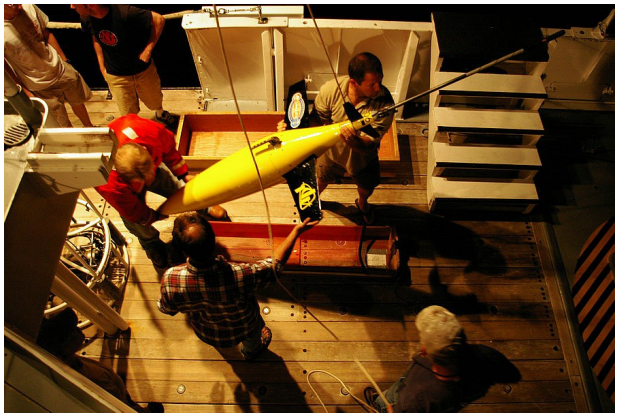

Figure7: Acoustic Seaglider being recovered (courtesy J. Curcio).

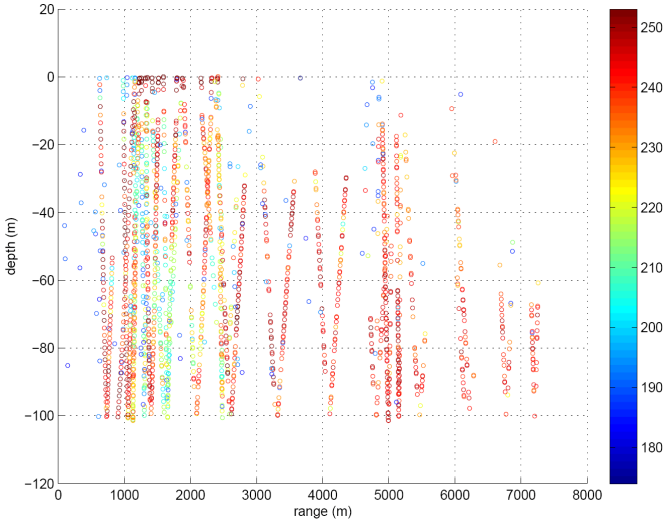

Figure 8: Signal quality versus range and depth. Signal quality ranges from 253 (high signal-to-noise ratio) to 100 (low SNR). One glider is sitting on the bottom communicating with another glider making multiple dives. Data from Puget Sound tests conducted summer 2007.

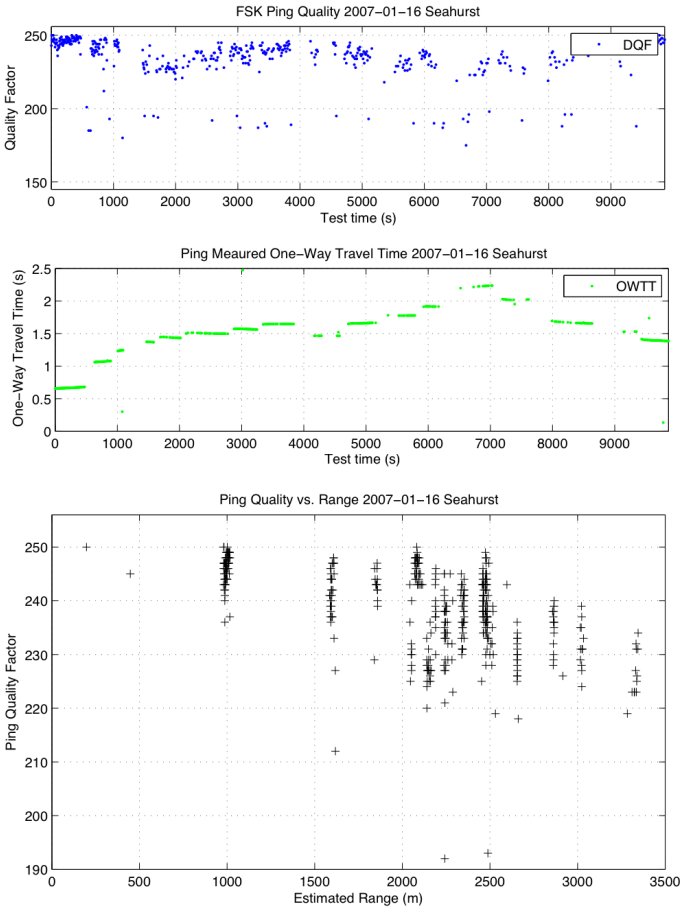

Figure 9: Acoustic modem results from Seahurst tests: (top) signal quality versus time, (middle) travel time versus time, (bottom) quality versus range.

C. Satellite Sensors

The space-based sensor that will be used in the adaptive sampling demonstration for this effort is the SeaWinds on the QuikSCAT mission. The SeaWinds scatterometer is a specialized microwave radar that measures near-surface wind velocity (both speed and direction) under all weather and cloud conditions over Earth's oceans. SeaWinds will collect data in a continuous 1,800-kilometer-wide band, making approximately 400,000 measurements and covering 90% of Earth's surface in one day. More information about the SeaWinds mission and its sensors can be found at: http://winds.jpl.nasa.gov/missions/quikscat/index.cfm

There are many other space-based sensors that can be used in this smart sensor web; these include JASON-1, OSTM, Aquarius, SWOT, and XOVWM.

D. Network Infrastructure

There is currently much activity within the oceanographic community to develop integrated underwater sensor networks that include mobile, fixed, autonomous, and cabled nodes. A significant difficulty in this effort is that the shallow underwater ocean environment is in general a very challenging medium in which to reliably communicate information. The reasons are well documented [3, 4]. Since

radio frequency (RF) waves attenuate extremely rapidly underwater, acoustic signaling is the preferred method of underwater wireless communication. Low acoustic sound speed introduces long propagation delays and extensive time spreading of the received signal. The shallow ocean environment is a dense scattering environment and is generally highly time varying. Acoustic signals attenuate very quickly as frequency increases; hence, the underwater channel is bandwidth limited. Furthermore, underwater Seagliders, such as those used in this project, are low power battery operated devices. This imposes practical constraints on the complexity of communications hardware [5].

Although the ocean presents significant challenges to communication, there has been considerable research into the physics of underwater acoustic propagation. The propagation of underwater sound is highly dependent upon the specific characteristics of the underwater channel. The primary sources of this dependence are the top and bottom surfaces as well as the acoustic sound speed profile (SSP). The SSP is the speed of sound with respect to depth. The dependence on the top surface is related to the surface roughness, while the dependence on the bottom surface also includes the specific characteristics of the bottom type (ie. sand, mud, clay, etc). The sound speed profile will affect the propagation of sound by causing a "bending" of the sound toward areas of lower sound speed [6].

The propagation of sound under water is governed by the wave equation; however, exact solutions to the wave equation are not possible for most practical underwater channels. An approximation to the wave equation is provided by Gaussian ray tracing. Gaussian ray tracing assumes that the source is composed of a fan of rays equally spaced in angle. The pressure due to each ray decays in a Gaussian fashion from the central beam of the ray. The propagation of each ray is governed by the ray equations, and the received power at a destination point can be determined from the superposition of the arriving rays [7].

Bellhop is a publicly available tool developed by the acoustics community that uses Gaussian ray tracing to give the transmission loss between a source and receiver pair in a user-defined underwater channel [8]. We can use the results of Bellhop to accurately characterize some fundamental attributes of the ocean environment as an information bearing medium.

Channel Capacity

The channel capacity is defined as the maximum rate of communication that a channel can support with asymptotically low probability of error. A fundamental result of information theory is that the capacity of a channel with additive white Gaussian noise (AWGN) is [9]:

$$C = B\log_2(1+\frac{P}{N_0 B}) \qquad (1)$$

where C is the capacity in bits/second, B is the channel bandwidth, P is the received power, and N_0 is the noise power spectral density.

However, the underwater channel is not AWGN, but is instead highly frequency selective. This frequency selectivity arises in two ways. The first is that the noise power spectral density is a function of frequency, and the second is that sound attenuates more strongly at higher frequencies according to Thorp's equation [10]:

$$10\log(a(f)) = 0.1\frac{f^2}{1+f^2} + 40\frac{f^2}{4100+f^2} \qquad (2)$$

where $10\log(a(f))$ is the attenuation at frequency f in dB/kilo-yard. Figure 10 plots this relationship for the frequency band between 10 and 100 kHz, scaling $10\log(a(f))$ to reflect db/km.

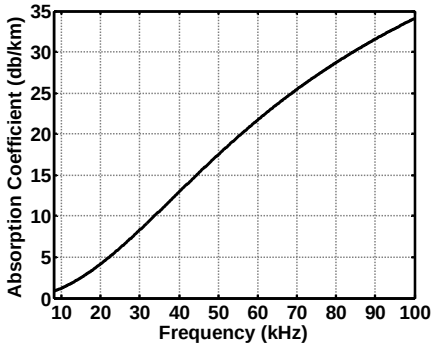

Figure 10: Absorption Coefficient in dB/kilometer.

The capacity of a frequency selective channel is defined by the following relationship [8]:

$$C = \sum_{\max P_n:\sum P_n \le P} B\log_2(1+\frac{|H_n|^2 P_n}{N_n B}) \qquad (3)$$

In this equation, the channel is divided into N 'bins' in frequency. The width of each bin is made sufficiently small such that the noise power, N_n, and the frequency response of the channel, $|H_n|^2$ can be considered uniform across the bin. The bandwidth B is then the bandwidth of each individual bin, so that the complete channel bandwidth is BN. The power is distributed across each bin in a way that maximizes the capacity of the channel, while maintaining the sum of the powers in each individual bin less than the total available power P. This procedure is typically called 'water filling' in frequency because the result mimics pouring of power into each frequency bin up to a certain level, with more power being poured into bins that are in a better state for communication (i.e., higher value of $|H_n|^2 / N_n$).

We use this procedure along with the results of Bellhop to determine the capacity of source and receiver pairs in specific underwater channels. We do this by determining the transmission loss from Bellhop for the given pair in small frequency bins. This allows us to capture the specific effects of the channel, including bottom and surface conditions as well as the SSP, in addition to the frequency selective absorption and noise given above. We use the results for transmission loss given by Bellhop for the values of $|H_n|^2$ in

the above equation, as well as a frequency selective noise model for the underwater environment given in [11].

Figure 11 gives the transmission loss profile in an underwater channel for sources at 10 m depth and 70 m depth. Figure 12 gives the capacity for receivers at different depths in each of these channels using equation (3). We can see that the capacity varies greatly between source and receivers pairs within the channel. For instance, in the lower plot of Figure 11, we can see that the drastic change in the SSP at approximately 30 m causes a condition where sound is trapped below this depth. This condition is reflected in the lower plot of Fig. 12, where the capacity is much greater for the receivers below 30 meters depth than for those above. These results indicate that within a water column, there is a clear advantage to transmitting with source/receiver pairs in specific locations within the column. We hope to exploit this relationship in future network structures.

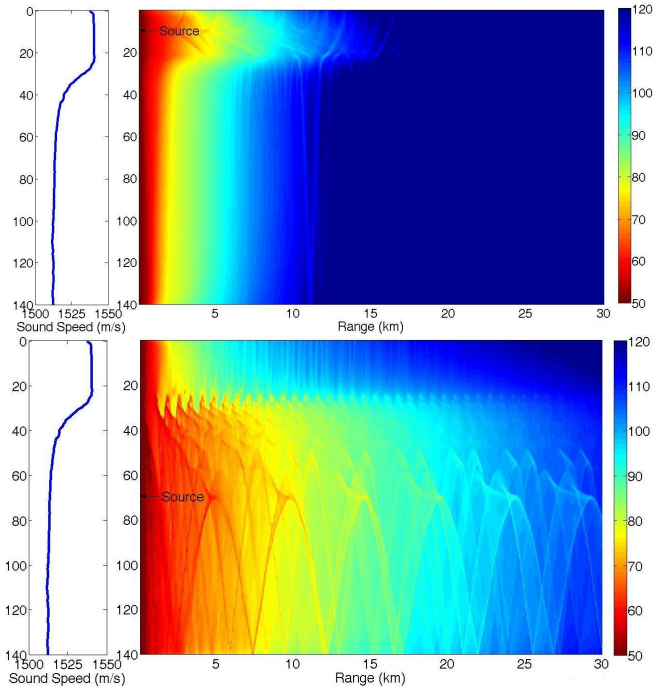

Figure 11: Transmission loss profile generated by Bellhop for a source at 10m (top) and 70m (bottom). The SSP is given to the left. The surface is modeled as having RMS wave height of 0.3 meters, and the bottom is modeled as 'medium sand'.

Network MAC Protocol

The challenges inherent to the underwater environment that we presented above also play a significant role in medium access control (MAC) protocol design. These primarily include the long propagation delay and bandwidth constraint that make common terrestrial MAC techniques unsuited to the underwater environment.

In order to overcome these challenges, we have developed a new MAC protocol that can be directly applied to the WHOI modem without changes to hardware or firmware and without the overhead of underwater localization or time synchronization. In keeping with the goal of practicality, we focus on a disciplined Aloha-type algorithm that exploits the available information of (expected) number of contending underwater nodes. The state transition diagram for the proposed MAC protocol is shown in Fig. 13. When a packet is received for transmission, a slot is chosen at random between 0 and CW-1. CW is the contention window, a network specific parameter that should be chosen based on the average number of contending nodes. The length of each slot is also a network specific parameter, which should be based on the maximum distance between nodes. When the packet for transmission is received at the MAC layer and a slot is chosen, a timer is set and begins counting down. Whenever a packet is heard on the channel, the MAC enters the receive state and the timer is paused until the MAC transitions to another state. When the timer reaches zero, the MAC transitions to the transmit (TX) state and the packet is transmitted. Upon completion of transmission, the MAC returns to the IDLE state.

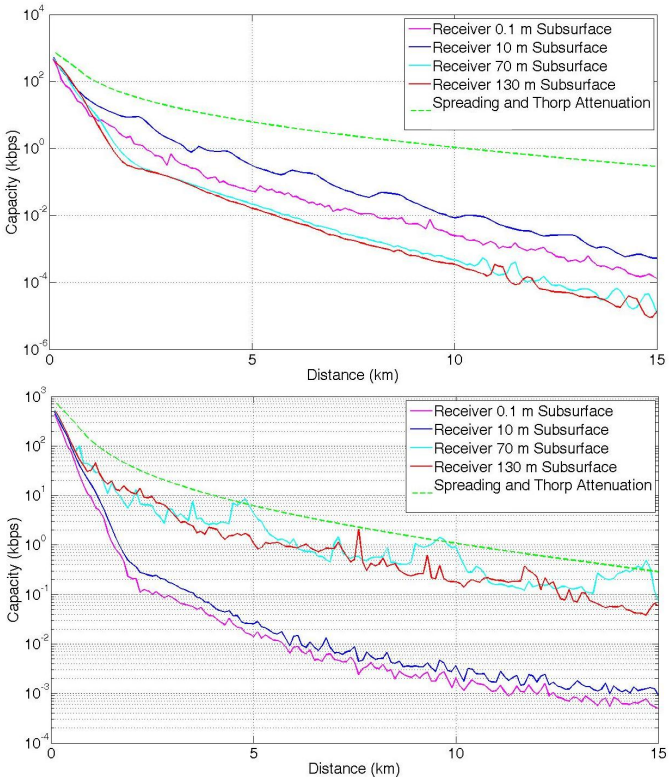

Figure 12: Capacity for the channels shown in Figure 11 top and bottom, with receivers at varying depth. The source power is 100 dB re 1 uPa, and the lowest frequency bin is centered at 7.5 kHz. The green line shows the capacity due to spreading and Thorp Attenuation alone.

In order to explore the benefit of the backoff mechanism on network throughput, we conducted *ns2* simulations for a network of varying numbers of nodes in a random topology. Nodes were randomly placed inside a square region at a depth of 50 m. Traffic generated at each of the nodes was destined for a receiver placed at the geographic center of the network area and placed at a depth of 30 m. This approximates an anticipated underwater acoustic network scenario where sensor nodes generate data for a central

gateway node. In all simulation runs, the packet length was assumed to be 3.2 seconds, the slot length was set to the maximum network propagation delay, and no retransmission scheme was employed. The WHOI Micromodem requires the successful reception of a cycle init packet prior to the transmission of a data packet. If the cycle init packet is missed or corrupted, the data packet will also be missed. We disregard the overhead added to packets and consider all transmitted data as useful data. The maximum achievable normalized throughput, therefore, is unity.

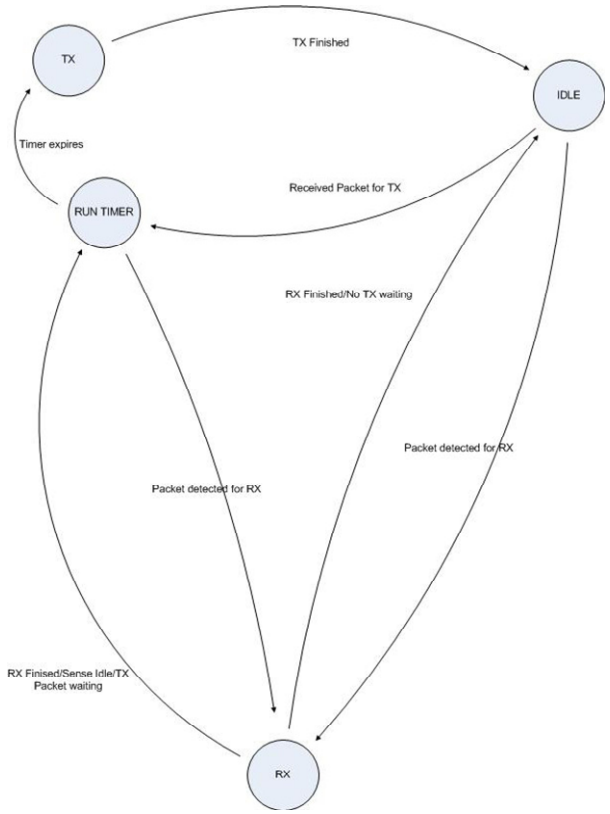

Figure 13: State transition diagram for MAC protocol.

Example 1: Saturated Traffic: The effects of the contention window size parameter, CW, were explored for 10, 15, and 20 nodes placed in a 250 km^2 grid while the value of CW was varied from 2 to 199. The nodes were saturated with data and the average throughput was measured. The results of 9 simulations were averaged for each value of CW. The simulation results shown in Fig. 14 demonstrate that the maximum achievable throughput is invariant to the number of nodes as long as CW is properly adjusted for the load.

Example 2: Poisson Traffic: We also conducted simulations with 15 nodes randomly placed in 40 km^2, 250 km^2, and 1000 km^2 square regions with the slot size set to the maximum possible propagation delay between nodes. Traffic was generated according to a Poisson assumption. The optimum value of CW was found through simulation in the same manner as previously discussed. Figure 15 shows the results of the simulation which demonstrate a substantial increase in throughput over a simple Aloha protocol. As expected, the maximum possible throughput is inversely proportional to the network size; however, even at longer ranges, throughput is increased. Figure 16 shows the percent of power wasted on collision for simulation runs of 10, 15, and 20 nodes in a 500 km^2 region, demonstrating that in addition to increased throughput, energy efficiency is improved by the backoff algorithm.

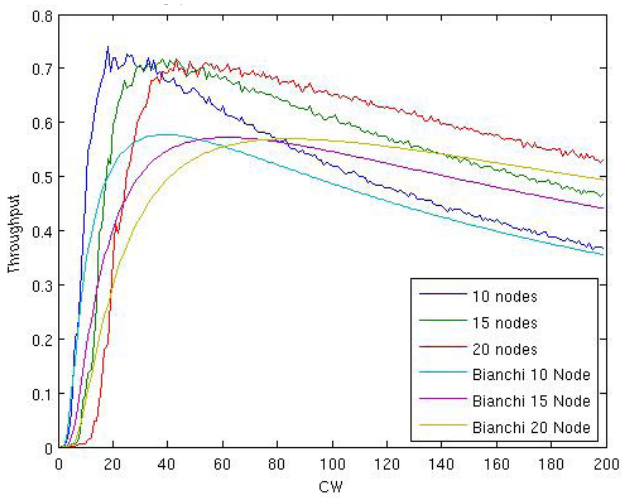

Figure 14: Throughput of saturated networks.

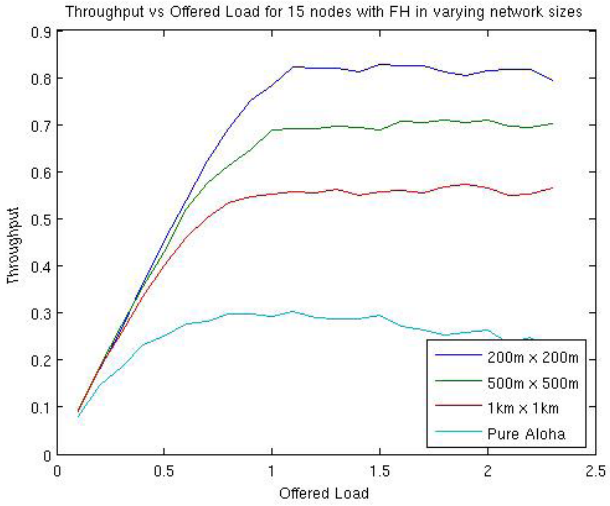

Figure 15: Throughput of varying network sizes under Poisson Traffic Assumption

Future Work

We have devised a MAC protocol that allows networks composed of WHOI Micromodems to move data with increased throughput and efficiency over a simple aloha scheme by implementing a backoff algorithm with knowledge of the expected number of contending nodes. While we are currently working on implementing the proposed network MAC protocol on the acoustic Seaglider, we are also working to develop new underwater acoustic communications techniques that will help improve underwater sensor webs to meet their theoretical potential.

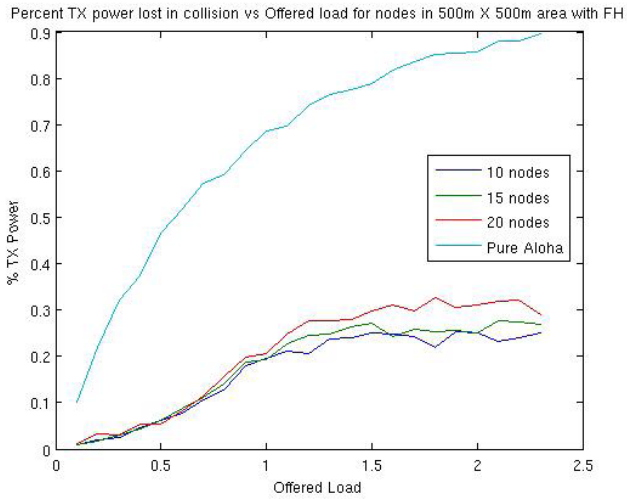

Figure 16: Power wasted in collision

E. Regional Ocean Modeling System (ROMS)

The in situ measurements, along with NASA satellite observations from Jason and QuikSCAT, will be used in a Regional Ocean Modeling System (ROMS) to realize the goal of adaptive sampling (Fig. 17). ROMS is a modeling infrastructure currently being developed (http://ourocean.jpl.nasa.gov/models.html) that solves the three-dimensional oceanic equations of momentum, temperature and salinity. ROMS also contains state-of-the-art parameterizations for surface boundary layer, turbulence mixing, and side boundary conditions. ROMS can be implemented in a multi-nested grid configuration that allows for telescoping from the large-scale down to local region at very high resolution (on the order of 1 km). ROMS also contains a three-dimensional data assimilation subsystem comprised of data quality control, model initialization and analysis, and forecasting components.

A 3-level nested ROMS model has been developed for the California Current System centered around the Monterey Bay (see Fig. 18). The spatial resolutions are 15-km, 5-km, and 1.5-km, respectively. This model can incorporate both satellite data and in-situ data obtained from the mooring sensor system and sensors on the Seagliders communicated via the underwater acoustic network.

This ROMS modeling and assimilation system has been tested twice during the field experiment in 2003 as part of the Autonomous Ocean Sampling Network II (AOSN-II) program (http://mbari.org/aosn) and again in 2006. During both field experiments, the ROMS modeling and data assimilation system was run daily in real-time, assimilating NASA satellite data including AVHRR, TOPEX/Poseidon and Jason as well as in-situ temperature and salinity data (e.g., derived from CTD measurements on moorings, ships, gliders, and autonomous underwater vehicles or AUVs). With the assimilated analysis as the initial condition and forced with the atmospheric model forecast, ROMS also made 3-day forecasts of all oceanographic variables. The results were posted on the project web site within 24 hours.

We are planning another field experiment either in Monterey Bay or Puget Sound. As part of the planned demonstration ambient sound measurements will hear whales, wind, rain, boats, ships, earthquakes, and fish. It might be feasible from the acoustic data to determine where whales are congregating. We will analyze the various signals, manually or automatically reconfigure the network, and navigate Seagliders to those locations for further investigation. Oceanographers can correlate these sound measurements with ocean properties (e.g. temperature & salinity).

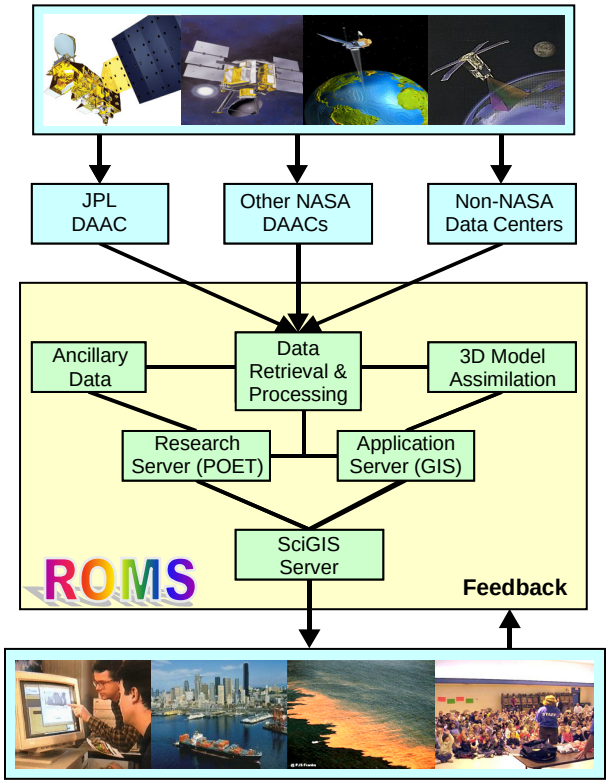

Figure 17: Schematic diagram of data flow from the sensor web to assimilation models to enable prediction and adaptive sampling.

The science and technical questions that our proposed experiment will address will include the following: How well can the gliders be navigated within this long-baseline system formed by the fixed modems (the mooring modems will have to be tracked relative to the bottom fixed modems)? How well is accurate and precise time maintained through the system? How much better could it be maintained with small changes? And; what is required to enable acoustic tomography over these small scales as well as larger scales (i.e., receiving distant sources)?

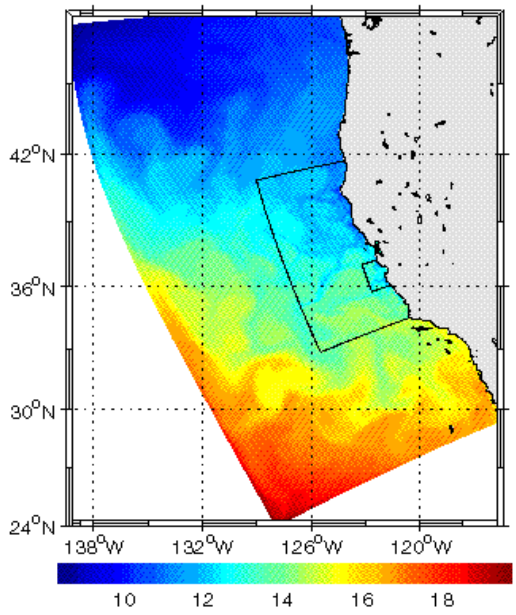

Figure 18: 3-level nested ROMS configuration centered around Monterey Bay, California.

III. Use Case

Here we present a high-level operational use case for the smart sensor web once it reaches operational readiness, achieved through completion of acoustic network technology development tasks and repeated integrated experiments as described previously. The use case presented here focuses on coastal disaster relief operations with a particular focus on search and rescue operations. In this scenario a sailor is lost at sea and the smart sensor web is used as part of the search and rescue effort.

The primary actors would be:

US Coast Guard
Search and rescue workers and volunteers

- Ships
- Planes
- Shore stations
- Computer analysts

Scientists (e.g. oceanographers) and technologists

- In-situ operators: boats, seagliders, underwater sensor networks
- Spacecraft operators
- Basic data processors (data-base maintenance, etc.)

Marine meteorologists

The assumed preconditions include:

- Access to real-time in situ and satellite data sets (e.g. QuickSCAT, Jason-1)
- Access to in-situ data sets (optional)
- Access to marine weather forecasts
- A well-calibrated ROMS model over a specific geographic region (e.g. California coastal ocean)
- Data and model forecast delivery mechanism to the end users (i.e. US Coast Guard)

The trigger event that starts the scenario is a 911 call in the evening reporting a missing sailor outside the Golden Gate of San Francisco Bay. The US Coast Guard would request operators of the Smart Ocean Sensor Web to assist and they would execute the following workflow:

1. Instrument operators instruct in-situ instruments (e.g. seagliders, ships, moorings) to obtain regional data
2. Scientists retrieve satellite data (e.g. ocean wind, sea height) from the NASA DAACs
3. Scientists run the COAMPS weather forecast model, from NRL, that produces wind prediction
4. Scientists preprocess data and perform data quality controls
5. Scientists run the 3D ocean model (ROMS model) to produce the preliminary results (e.g. sea level, wind)
6. Scientists perform data assimilation to improve the first estimate by adding a correction based on the model and data misfit
7. Make predictions of ocean surface current (and other oceanographic variables) up to 48 hours into the future
8. Process the model forecast data and make images
9. Distribute the model forecast to the end users (i.e., US Coast Guard)

The US Coast Guard and Research and Rescue Operations would perform the following:

1. Based on the ROMS Ocean forecast, the US Coast Guard will estimate the search area over the next 24 hours (e.g. develop such things as error ellipses over lat/long maps etc.)
2. The research and rescue workers will plan (temporally and spatially) the resources (e.g., ships, planes, people) needed to implement the research and rescue operation
3. Rescue workers perform rescue operations

These processes are repeated daily until the missing sailor is found. The environmental information provided to the US Coast Guard and their impact to guide the search and rescue operations will be archived for post-operation analysis with a goal to improve models, data assimilation schemes, and the marine weather and ocean forecast.

IV. Concluding Remarks

The sensor web presented here achieves traceability to science through complementing existing and planned space science missions. Specifically the sensor web integrates space-based sensor data with in-situ data; these are integrated via the ROMS model, the output of which can used for achieving a set of scientific objectives, including enhancing the science products of stand-alone missions:

- QuikSCAT
- Jason-1
- OSTM

- Aquarius
- SWOT
- XOVWM

The output of the ROMS model is also useful in planning future space-based missions (investment) dedicated to climate change science. As demonstrated through a use case the sensor web will also be useful for coastal disaster relief operations, in particular search and rescue operations.

In conclusion, the ocean-observing smart sensor web presented herein was composed of (a) a cable-connected mooring system with a profiler under real-time control with inductive battery charging; (b) a glider with integrated acoustic communications and broadband receiving capability; (c) satellite sensor elements; (d) an integrated acoustic navigation and communication network; and (e) a predictive model via the Regional Ocean Modeling System (ROMS). The acoustic communications network forms a critical link in the web between the in-situ and space-based sensors and facilitates adaptive sampling and calibration.

ACKNOWLEDGMENTS

This work reported here is funded by three projects. The integrated underwater/satellite sensor network science and technology development is funded by the NASA Earth Science Technology Office's Advanced Information Systems Technology (AIST) Program under award number AIST-05-0030. The mooring work is funded by the National Science Foundation (NSF) Ocean Technology and Interdisciplinary Coordination (OTIC) program, Grant OCE 0330082. The acoustic Seaglider work is funded by the Office of Naval Research (ONR), Grant N00014-05-1-0907. Thanks are given to the many scientists and engineers who have contributed to this work.

REFERENCES

[1] C. Wunsch, R. Ponte and P. Heimbach, "Decadal trends in sea level patterns", *J. Clim.* vol. 2024, pp. 5889–5911, 2007.

[2] B.M. Howe, P, Arabshahi, W. L. J. Fox, S. Roy, T. McGinnis, M. L. Boyd, A. Gray, and Yi Chao, "A smart sensor web for ocean observation: system design, architecture, and performance," *Proc. 2007 NASA Science Technology Conference*, University of Maryland, June 19-21, 2007.

[3] M. Stojanovic, "Recent advances in high-speed underwater acoustic communication," *IEEE J. Oceanic Eng*., vol. 21, pp 125-136, 1996.

[4] D.B. Kilfoyle and A.B. Baggeroer, "The state of the art in underwater acoustic telemetry," *IEEE J. Oceanic Eng.*, vol. 25, pp 4-27, 2000.

[5] S. Roy, P. Arabshahi, D. Rouseff and W. Fox, "Wide area ocean networks: architecture and system design considerations," *Proc. 1st ACM International workshop on Underwater networks*, 2006.

[6] R.J. Urick, *Principles of Underwater Sound, 3rd ed.* New York: McGraw Hill, 1983.

[7] F.B. Jensen, W. B. Kuperman, M. B. Porter and H. Schmidt, *Computational Ocean Acoustics*. Woodbury, NY: AIP Press, 1994.

[8] M.B. Porter (2007) Bellhop Gaussian beam/finite element beam code. http://oalib.hlresearch.com/Rays/index.html.

[9] A. Goldsmith, *Wireless Communications*. New York, NY: Cambridge University Press, 2005.

[10] W.H. Thorp, "Analytic description of the low-frequency attenuation coefficient," *J. Acoustical Soc. of America*, vol. 42, p. 270, 1967.

[11] R. Coates, *Underwater Acoustic Systems*. New York: John Wiley and Sons, 1989.